SLAC-PUB-2296
March 1979
(T/E)

TOPICS IN THE QCD PHENOMENOLOGY OF DEEP - INELASTIC SCATTERING

L. F. Abbott

Stanford Linear Accelerator Center
Stanford University, Stanford, California 94305

ABSTRACT

I review the status of QCD with respect to recent results from deep - inelastic neutrino scattering, emphasizing the theoretical uncertainties coming from effects of non-leading order in $1/Q^2$ and in α_s.

(Invited talk presented at the Orbis Scientiae, University of Miami, Coral Gables, Florida , January 15 - 19, 1979.)

* Work supported by the Department of Energy under contract number EY-76-C-03-0515.

I. INTRODUCTION

During the past year, new results from neutrino experiments[1,2] have been compared with QCD predictions for scaling violations in deep-inelastic structure functions.[1-4] Good agreement between theory and experiment has been found. In what sense do these comparisons test QCD? To answer this question we must examine the various theoretical uncertainties involved in making the QCD predictions. The basic QCD calculations for deep-inelastic scattering,[5] which are discussed in Section II, treat only the lowest-twist operators in the operator product expansion and only leading-order terms in the QCD coupling parameter α_s. As a result, there are corrections of order $1/Q^2$, $1/Q^4$, etc., coming from target mass effects and from higher-twist operators, and corrections which are higher order in α_s. Target mass effects can be taken into account,[6-8] but the effects of higher-twist operators remain as a source of uncertainty for predictions at low Q^2. These issues are discussed in Section III. The corrections of second order in α_s to the leading-order QCD results have now been computed.[9] Their phenomenological implications are discussed in Section IV. The work described here was done in collaboration with Michael Barnett.

II. HIGH-Q^2 RESULTS

Two effects which are higher order in $1/Q^2$, elastic scattering contributions and target mass effects, can be directly measured. Using BEBC-Gargamelle data,[1] we find that for analyses of the Q^2-evolution of xF_3, or of moments of xF_3 for $N \lesssim 6$ both of these

effects are smaller than the experimental errors for $Q^2 > 3\ \mathrm{GeV}^2$. We therefore think it reasonable to assume that other effects of higher-twist operators are also small for $Q^2 > 3\ \mathrm{GeV}^2$.

In order to compare QCD with neutrino data, I will use the QCD equations for the Q^2- evolution of deep-inelastic structure functions.[5,10] For the non-singlet structure function xF_3 the evolution equation is particularly simple. Defining

$$xF_3\ (x,Q^2) \;=\; F\ (x,Q^2) \tag{2.1}$$

we have

$$Q^2\,\frac{\partial F\ (x,Q^2)}{\partial Q^2} \;=\; \frac{\alpha_s\ (Q^2)}{3\pi}\left\{\Big(3 + 4\ \ell n\ (1-x)\Big)F\ (x,Q^2) + \int_x^1 dz\ \frac{2}{(1-z)}\left[(1+z^2)\ F\left(\frac{x}{z},\,Q^2\right) - 2F\ (x,Q^2)\right]\right\} \tag{2.2}$$

where

$$\alpha_s\ (Q^2) \;=\; \frac{12\ \pi}{(33-2n_f)\ \ell n\ Q^2/\Lambda^2} \tag{2.3}$$

for n_f quark flavors. In order to proceed, along with Eq. (2.2) one must specify a boundary condition for $F\ (x,Q^2)$ at some reference point $Q^2 = Q_0^2$. This boundary condition is not completely specified by QCD calculations. We take the standard parameterization

$$F\left(x,Q_0^2\right) \;=\; A x^a\ (1-x)^b \tag{2.4a}$$

and, following the CDHS group,[2] we use the values

$$\begin{aligned} Q_0^2 &= 20\ \text{GeV}^2 \\ A &= 3.3 \\ a &= .5 \\ b &= 3 \end{aligned} \tag{2.4b}$$

Then, integrating Eq. (2.2) we obtain the solid curves in Figs. 1 - 4. The data points shown are a weighted average of BEBC - Gargamelle[1] and CDHS[2] results. Fig. 1 shows the initial fit of Eq. (2.4) to the combined data at $Q^2 = 20\ \text{GeV}^2$. This initial fit is also shown for reference in Figs. 2 - 4 by the dashed curve. The curves predicted by QCD on the basis of the initial fit are shown in Figs. 2 and 3 for $Q^2 = 64\ \text{GeV}^2$ and for $Q^2 = 100\ \text{GeV}^2$. The agreement between theory and experiment is quite striking. Fig. 4, showing the QCD fit at $Q^2 = 3.9\ \text{GeV}^2$, is less dramatic but still in reasonable agreement.

In Figs. 1 - 4, we have combined BEBC - Gargamelle[1] and CDHS[2] data. It should be pointed out that at high Q^2 there is some disagreement between the two data sets, where they overlap, in the range $.5 \leq x \leq .7$. The effects of this discrepancy are minor in the plots I have shown. However, if one takes moments for the two data sets one weights the range of x where the discrepancy occurs heavily and the disagreement for the moments becomes quite large. Another important point is that the Q^2 - evolution of $F(x,Q^2)$ at some particular $x = x_0$ depends on $F(x,Q^2)$ only for $x \geq x_0$. Thus, although $F(x,Q^2)$ is not well determined by the data for small x, this uncertainty does not feed through the equations to larger x values.

III. EFFECTS OF HIGHER ORDER IN $1/Q^2$

For $Q^2 < 3\ GeV^2$, terms of higher order in $1/Q^2$ are important. This can be seen by the presence of a large elastic-scattering contribution and of sizeable target mass corrections as will be shown below. Terms of higher order in $1/Q^2$ arise from both kinematics and dynamics. Kinematic effects come from the finite target mass, $p^2 = m^2$ where p is the target momentum; and from finite hadronic masses in the final state, $W^2 \geq m^2$ where W is the final-state hadronic mass. Dynamical effects include elastic scattering, resonance formation, diquark scattering, constituent pion scattering, transverse momentum effects and many others. Of these, only the target mass effects can be correctly incorporated into the QCD predictions.

Target mass corrections are made by using the ξ - scaling variable[7,8] or equivalently by taking Nachtmann moments.[6] First, I will discuss the ξ variable within the context of the parton model,[8] and then I will discuss mass corrections in the operator product expansion[7] and Nachtmann moments.[6] The two discussions are equivalent and reflect two ways of looking at the same problem, but it is instructive to state both of them.

Consider the target nucleon momentum parameterized in the convenient form[11]

$$p_{nucleon} = \left(P + \frac{m^2}{4P},\ \vec{0},\ P - \frac{m^2}{4P}\right) \tag{3.1}$$

This form guarantees that $p^2_{nucleon} = m^2$.

Then, let the initial momentum of the struck quark be

$$p_{quark} = \left(xP + \frac{\vec{k}_\perp^{\,2}}{4xP}, \ \vec{k}_\perp, \ xP - \frac{\vec{k}_\perp^{\,2}}{4xP} \right) \tag{3.2}$$

This quark is taken to be massless. Note that

$$x = \frac{(p_0 + p_3)_{quark}}{(p_0 + p_3)_{nucleon}} \tag{3.3}$$

The final momentum of the struck quark is $(p_{quark} + q)$. If it too is massless, we have the condition

$$(p_{quark} + q)^2 = 0 \tag{3.4}$$

Solving this equation ignoring $\vec{k}_\perp$ gives the ξ scaling variable

$$x = \xi = \frac{\nu}{m}\left[\sqrt{1 + \frac{Q^2}{\nu^2}} - 1\right] \tag{3.5}$$

where

$$m\nu = q \cdot p_{nucleon} \tag{3.6}$$

To take target-mass effects into account for xF_3 one would leave Eqs. (2.2 - 2.4) unchanged, but Eq. (2.1) would be replaced by

$$xF_3(x,Q^2) = \frac{x^2}{\xi^2}\frac{1}{\left(1+\frac{4m^2x^2}{Q^2}\right)}F(\xi,Q^2) + \frac{4m^2}{Q^2}\frac{x^3}{\left(1+\frac{4m^2x^2}{Q^2}\right)^{3/2}}\int_\xi^1 d\xi'\left[\frac{F(\xi',Q^2)}{(\xi')^2}\right] \tag{3.7}$$

A second derivation of ζ- scaling starts with the operator product expansion of two currents (suppressing vector indices of the currents J)

$$J(x)\,J(0) \;=\; \sum_{i} \sum_{J} \left[C_J^i(x^2) x_{\mu_1} \cdots x_{\mu_J} \, O^{i,J}_{\mu_1 \cdots \mu_J} \right] \tag{3.8}$$

where the $O^{i,J}_{\mu_1 \cdots \mu_J}$ are local operators of spin J. If we ignore the target mass ($p^2 = 0$) and write the nucleon matrix elements of the operator $O^{i,J}_{\mu_1 \cdots \mu_J}$ as

$$\langle p \mid O^{i,J}_{\mu_1 \cdots \mu_J} \mid p \rangle \;=\; A_J^i \left[p_{\mu_1} \cdots p_{\mu_J} \right] \tag{3.9}$$

then the tensors $[p_{\mu_1} \cdots p_{\mu_J}]$ are symmetric and traceless forming irreducible tensors of O(4). However, if we take the target mass into account ($p^2 = m^2$) these tensors are reducible due to their non-vanishing traces. Since the operator $O^{i,J}_{\mu_1 \cdots \mu_J}$ has definite spin we must write

$$\langle p \mid O^{i,J}_{\mu_1 \cdots \mu_J} \mid p \rangle \;=\; A_J^i \Big[p_{\mu_1} \cdots p_{\mu_J} - \frac{m^2}{4} g_{\mu_1\mu_2} p_{\mu_3} \cdots p_{\mu_J} - \text{all other traces} \Big] \tag{3.10}$$

This modification leads to the ξ scaling variable[7] and to Nachtmann moments[6]

$$\tilde{M}_N \;=\; \int_0^1 dx \; \frac{\xi^{N+1} x F_3(x,Q^2)}{x^3} \left[\frac{1 + (N+1)\sqrt{1 + \frac{4m^2x^2}{Q^2}}}{(N+2)} \right] \tag{3.11}$$

to replace the simple moments

$$M_N = \int_0^1 dx\ x^{N-2}\ xF_3(x,Q^2) \tag{3.12}$$

Although the ξ-scaling scheme correctly accounts for target mass effects, it does not correctly describe the final-state kinematics in deep-inelastic scattering.[12] Kinematics requires that xF_3 vanishes at $x = 1$ and quark counting rules[13] suggest a form like $(1-x)^3$ near $x = 1$. When the ζ scaling variable is used, $(1-x)^3$ gets replaced by $(1-\xi)^3$ and at $Q^2 = 1\ \text{GeV}^2$, for example, $x = 1$ corresponds to $\xi = .64$. As a result, xF_3 does not vanish at $x = 1$ in the ξ-scaling scheme. In the above parton model derivation, we have taken $p^2 = m^2$ for the initial nucleon momentum but have ignored the final-state kinematic condition $W^2 \geq m^2$. For example, if we included non-zero final-state hadronic masses we could not have taken the initial quark on mass shell as in Eq. (3.2). Thus, the ξ-scaling scheme assumes that the dominant $1/Q^2$ effects can be removed by correcting the initial-state kinematics only and ignoring final-state kinematics and dynamical effects. This is somewhat supported by the fact that the ξ-scaling variable acts much like the scaling variable of Bloom and Gilman.[14] In overshooting the data near $x = 1$, one can argue[15] that ξ-scaling accounts for the elastic scattering contribution (and resonance contributions) in the sense that the excess area under the ξ-scaling curve equals the area under the elastic peak at $x = 1$.

The key issue is then: once target mass corrections have been made, how large are the remaining higher-twist effects. This is an

extremely difficult question to answer. We have fit the BEBC-Gargamelle data[1] for moments of xF_3 to the form

$$\tilde{M}_N = M_N^{QCD}\left[1 + \frac{aN}{Q^2}\right] \tag{3.13}$$

where $\tilde{M}_N$ is a Nachtmann moment and M_N^{QCD} is the QCD prediction. The factor of N in the $1/Q^2$ term is suggested by quark counting rules.[13] Fixing the Λ parameter of QCD from the high Q^2 data we find $a \approx .2$ GeV^2. However, if the Λ parameter is not held fixed we find that the data do not distinguish between $1/Q^2$ and $1/\ell nQ^2$ effects, and in fact this question cannot be resolved. The inclusion of other terms like $1/Q^4$, $1/Q^6$, $1/Q^8$, etc., does not change the situation.

Figure 5 shows the effects of elastic scattering and of the target mass at $Q^2 = 1.7$ GeV^2. The dashed curve is the x-scaling prediction of QCD obtained by integrating the QCD evolution equation for xF_3, Eq. (2.2), down from the initial fit of Eq. (2.4) at $Q^2 = 20$ GeV^2, and using Eq. (2.1) to define xF_3. The solid curve is the corresponding ξ-scaling prediction obtained from Eq. (3.7). The elastic data which is actually a sharp spike at x = 1 is displayed by adding on extra bin from x = 1 to x = 1.1. The area under the data point in this bin is equal to the area under the elastic peak in the original data. Note that the elastic contribution is quite large and that the difference between the x-scaling and ξ-scaling curves is substantial. This shows the presence of significant corrections of higher order in $1/Q^2$. The x-scaling (dashed) curve fits quite well in the large x region except for the elastics. This suggests that the simple moments of Eq. (3.12)

excluding elastics would agree well with QCD which is in fact true. The ξ - scaling curve overshoots the data at large x but the area between the ξ - scaling curve and the x - scaling curve is approximately equal to the area under the elastic peak. This suggests that the Nachtmann moments of Eq. (3.11) including elastics would also agree well with QCD. Again this is true. ~~In~~ considering which curve in Fig. 5 fits better, it is not at all clear what one means by a good fit a low Q^2. At present the data is not precise enough to distinguish between $1/Q^2$ and $1/\ell nQ^2$ effects. Thus, low Q^2 data cannot be used to test QCD until more is known about higher-twist effects. On the other hand, it does contain information which may be helpful in resolving these issues in the future.

IV. EFFECTS OF HIGHER ORDER IN α_s

Figure 6 shows a comparison of the BEBC - Gargamelle data[1] for the N = 3 Nachtmann moment with the leading order QCD prediction

$$\tilde{M}_N = \frac{C_N}{\left(\ell n\ Q^2/\Lambda^2\right)^{d_N}} \tag{4.1}$$

where the d_N are known parameters and the constants C_N and Λ are determined by fitting to the data. We have already seen that the QCD prediction for $Q^2 < 3\ GeV^2$ is subject to uncertainties due to effects of higher order in $1/Q^2$. There are also uncertainties coming from terms of higher order in α_s. The corrections of second - order in α_s

change Eq. (4.1) to[9]

$$\tilde{M}_N = \frac{C_N}{\left(\ell n\ Q^2/\Lambda^2\right)^{d_N}} \left[1 + \frac{A_N + B_N\, \ell n\, \ell n\ Q^2/\Lambda^2}{\ell n\ Q^2/\Lambda^2}\right] \qquad (4.2)$$

The constants A_N and B_N have now been computed.[9] We can then fit Eq. (4.2) to the data of Fig. 6 again varying C_N and Λ to obtain the best fit. We find that although the correction terms are large, the curve obtained using Eq. (4.2) is virtually identical to the curve we found by fitting with Eq. (4.1). This is because the effect of the second-order corrections can almost entirely be absorbed into a renormalization of the parameter Λ.[3] The large second-order corrections change the value of Λ dramatically but have a very small effect on the curve of Fig. 6. This is true for moments over a small range of N (say $2 \leq N \leq 6$) but is no longer valid if we try to fit over a large range of N. Recently, Ross[16] has shown that the large second-order corrections to the QCD curves of xF_3 (Figs. 1-4) occur at large and small x. At large x since xF_3 vanishes this is not too critical and at small x the fit to xF_3 is poorly known anyway. Thus, the second-order corrections and hopefully all corrections of higher-order in α_s do not introduce too much uncertainty into qualitative QCD predictions such as those of Figs. 1 - 6.

However, the second-order corrections in α_s do present a problem when we go beyond curve fitting and try to give numerical predictions from QCD. For example, the BEBC - Gargamelle group[1] has obtained a

parameter r by requiring

$$\frac{d}{dQ^2}\left(\frac{M_N^r}{M_M}\right) = 0 \qquad (4.3)$$

Using the lowest-order form of Eq. (4.1) we see that QCD predicts that Eq. (4.3) can be satisfied at all Q^2 with

$$r = \frac{d_M}{d_N} \qquad (4.4)$$

To include the second-order corrections in α_s,[4] we must substitute Eq. (4.2) into Eq. (4.3). We find that Eq. (4.3) can no longer be satisfied at all Q^2 but that it can be satisfied at one Q^2 value and then is very nearly satisfied at all other Q^2 values in the experimental range. However, the QCD prediction for r is now quite different from the leading-order prediction of Eq. (4.4). For example, if we choose to satisfy Eq (4.3) at $Q^2 = 5\ \text{GeV}^2$ (the values given are not very sensitive to this choice) and take $\Lambda = .5$ GeV, we obtain the following results

TABLE I

QCD Prediction

M/N	r(Leading-Order)	r(Second-Order)
5/3	1.46	1.74
6/4	1.29	1.46
7/3	1.76	2.28

Thus, the parameter r is subject to quite large corrections due to effects of higher order in α_s.[4]

The calculations of the second-order corrections to the moments also serve to point out ambiguities in the definitions of α_s and Λ.[3,17,18] First, α_s can only be defined by specifying a renormalization scheme. Two α_s parameters defined in two different schemes disagree at second-order and are related by

$$\alpha_s' = \alpha_s + \alpha_s^2 + \ldots \tag{4.5}$$

However, even if the renormalization scheme is fixed, there is still an arbitrariness in the definition of Λ which results in an ambiguity exactly like Eq. (4.5). Consider some function expanded in powers of $1/\ell n\ Q^2$

$$F = \frac{A}{\ell n\ Q^2/\Lambda^2} + \frac{B}{\ell n^2 Q^2/\Lambda^2} + \ldots \tag{4.6}$$

Now define

$$\Lambda_a = \Lambda e^{\frac{1}{2}a} \tag{4.7}$$

Then,

$$\frac{1}{\ell n\ Q^2/\Lambda^2} = \frac{1}{\ell n\ Q^2/\Lambda_a^2} - \frac{a}{\ell n^2 Q^2/\Lambda_a^2} + \ldots \tag{4.8}$$

and we can write

$$F = \frac{A}{\ell n\ Q^2/\Lambda_a^2} + \frac{B-a}{\ell n^2 Q^2/\Lambda_a^2} + \ldots \tag{4.9}$$

Thus, we have the possibility of expanding using different Λ's and getting different values of the constant in the second-order term.

If we use the definition of Λ_a in Eq. (4.7) for the moments of Eq. (4.2), we find[3]

$$\tilde{M}_N = \frac{C_N}{\left(\ell n\ Q^2/\Lambda_a^2\right)^{d_N}} \left[1 + \frac{A_N - a d_N + B_N\, \ell n \ell n\ Q^2/\Lambda_a^2}{\ell n\ Q^2/\Lambda_a^2}\right] \qquad (4.10)$$

Note therefore, that one cannot define Λ without specifying the constant term in the second-order correction nor can one say how large the second-order term is without defining what definition of Λ is being used.

In fitting the second-order QCD prediction for the moments to data, one must decide what Λ to use and hence what value of the constant term in the second-order correction to fit with. There are several possible approaches. The calculations of the A_N and B_N were done in the minimal subtraction scheme using dimensional regularization. The A_N contain factors of $\ell n\,(4\pi) - \gamma_E$ coming from expanding around $n = 4$ in the dimensional regularization method. Since these factors are artifacts of the regularization scheme, one can choose[3]

$$a = \ell n\,(4\pi) - \gamma_E \approx 2 \qquad (4.11)$$

in order to remove such factors from the A_N. Another approach is to choose a value of a so that the second-order term is as small as possible over the Q^2 range and for the moments of interest.[3,4] This also leads to an a close to two. Finally, we have fit Eq. (4.10) using C_N, Λ_a, and a all as free parameters. We find $a = 2.3 \pm .6$ but this determination can only be made using low Q^2 data where effects of higher order in $1/Q^2$ introduce uncertainties. It is interesting that all three methods lead to roughly the same value of a.

The best definitions of α_s and Λ to use are clearly those which minimize the effects of higher-order corrections. The results of the last paragraph suggest that at moderate Q^2 values, for moments $2 \leq N \leq 6$ the best choice might be $a \approx 2$ in Eq. (4.10). The second-order corrections to the total e^+e^- cross section are now being computed. It will be interesting to see whether the definitions of α_s and Λ which seem to be best in deep-inelastic scattering also minimize the effects of second-order corrections to electron-positron annihilation.

Finally, I would like to point out that in comparing values of Λ or α_s from different processes, one must be sure that the same definitions of these parameters are being used. This can only be done if the second-order corrections are known. In particular, there is no meaning to comparisons of Λ's obtained from different processes using the lowest-order results of QCD.[17]

ACKNOWLEDGMENTS

This work was done in collaboration with Michael Barnett, I am extremely grateful to many colleagues and in particular to R. Blankenbecler, S. Brodsky and F. Gilman for helpful conversations.

This research was supported by the Department of Energy under contract number EY-76-C-03-0515.

REFERENCES

1. P. Bosetti et al., Nucl. Phys. B142, 1 (1978).

2. J. G. H. de Groot et al., CERN preprints 79-0168, 79-0132 and 79-0133.

3. W. A. Bardeen, A. J. Buras, D. W. Duke and T. Muta, Phys. Rev. D18, 3998 (1978).

4. R. Barbieri, L. Caneschi, G. Curci and E. d'Emilio, preprint SNS 8/1978.

5. Some reviews are H. D. Politzer, Phys. Reports 14C, 129 (1974); D. J. Gross in Methods in Field Theory, ed. R. Balian and J. Zinn-Justin (North-Holland, 1976); J. Ellis in Weak and Electromagnetic Interactions at High Energy, ed. R. Balian and C. H. Llewellyn-Smith (North-Holland, 1977).

6. O. Nachtmann, Nucl. Phys. B63, 237 (1973); B78, 455 (1974); S. Wandzura, Nucl. Phys. B42, 412 (1977).

7. H. Georgi and H. D. Politzer, Phys. Rev. D14, 1829 (1976).

8. R. Barbieri, J. Ellis, M. K. Gaillard and G. G. Ross, Phys. Lett. 64B, 171 (1976); Nucl. Phys. B117, 50 (1976); R. K. Ellis, R. Petronzio and G. Parisi, Phys. Lett. 64B, 97 (1976).

9. W. Caswell, Phys. Rev. Lett. 33, 244 (1974); D. R. T. Jones, Nucl. Phys. B75, 531 (1974); E. G. Floratos, D. A. Ross and C. T. Sachrajda, Nucl. Phys. B129, 66 (1977); Erratum B139, 545 (1978); CERN preprints TH-2566 and TH-2570; W. A. Bardeen, A. J. Buras, D. W. Duke and T. Muta, Phys. Rev. D18, 3998 (1978).

10. G. Altarelli and G. Parisi, Nucl. Phys. B126, 298 (1977).

11. D. Sivers, S. Brodsky and R. Blankenbecler, Physics Reports 23C, 1 (1976).

12. D. J. Gross, F. A. Wilczek and S. B. Treiman, Phys. Rev. D15, 2486 (1976); K. Bitar, P. W. Johnson and W-K Tung, IIT preprint.

13. S. Brodsky and G. Farrar, Phys. Rev. Lett. 31, 1153 (1973); Phys. Rev. D11, 1309 (1975); R. Blankenbecler and S. Brodsky, Phys. Rev. D10, 2973 (1974).

14. E. Bloom and F. Gilman, Phys. Rev. Lett. 25, 1140 (1970).

15. A. DeRujula, H. Georgi and H. D. Politzer, Ann. Phys. 103, 315 (1977).

16. D. A. Ross, Caltech preprint 68-699.

17. M. Bacé, Phys. Lett. 78B, 132 (1978).

18. S. Wolfram, Caltech preprint 68-690; W. Celmaster and R. J. Gonsalves, UCSD preprint 10P10-210.

FIGURE CAPTIONS

Fig. 1. A fit of the form $xF_3 = Ax^a(1-x)^b$ to the combined BEBC - Gargamelle and CDHS data at $Q^2 = 20$ GeV^2.

Fig. 2. The solid curve is the QCD prediction for xF_3 based on the fit of Fig. 1 which is reproduced here as the dashed curve. The data is combined BEBC - Gargamelle and CDHS results at $Q^2 = 64$ GeV^2.

Fig. 3. Same as Fig. 2 but at $Q^2 = 100$ GeV^2.

Fig. 4. Same as Fig. 2 but at $Q^2 = 3.9$ GeV^2.

Fig. 5. The dashed curve is the x - scaling prediction of QCD based on the initial fit at $Q^2 = 20$ GeV^2 of Fig. 1. The solid curve is the corresponding ξ - scaling prediction. Data is from BEBC - Gargamelle and elastics are shown in a bin from $x = 1$ to $x = 1.1$ where the area under the data point in this bin is equal to the area under the elastic peak at $x = 1$ in the original data.

Fig. 6. A comparison of the QCD prediction with the $N = 3$ Nachtmann moment from the BEBC - Gargamelle data.

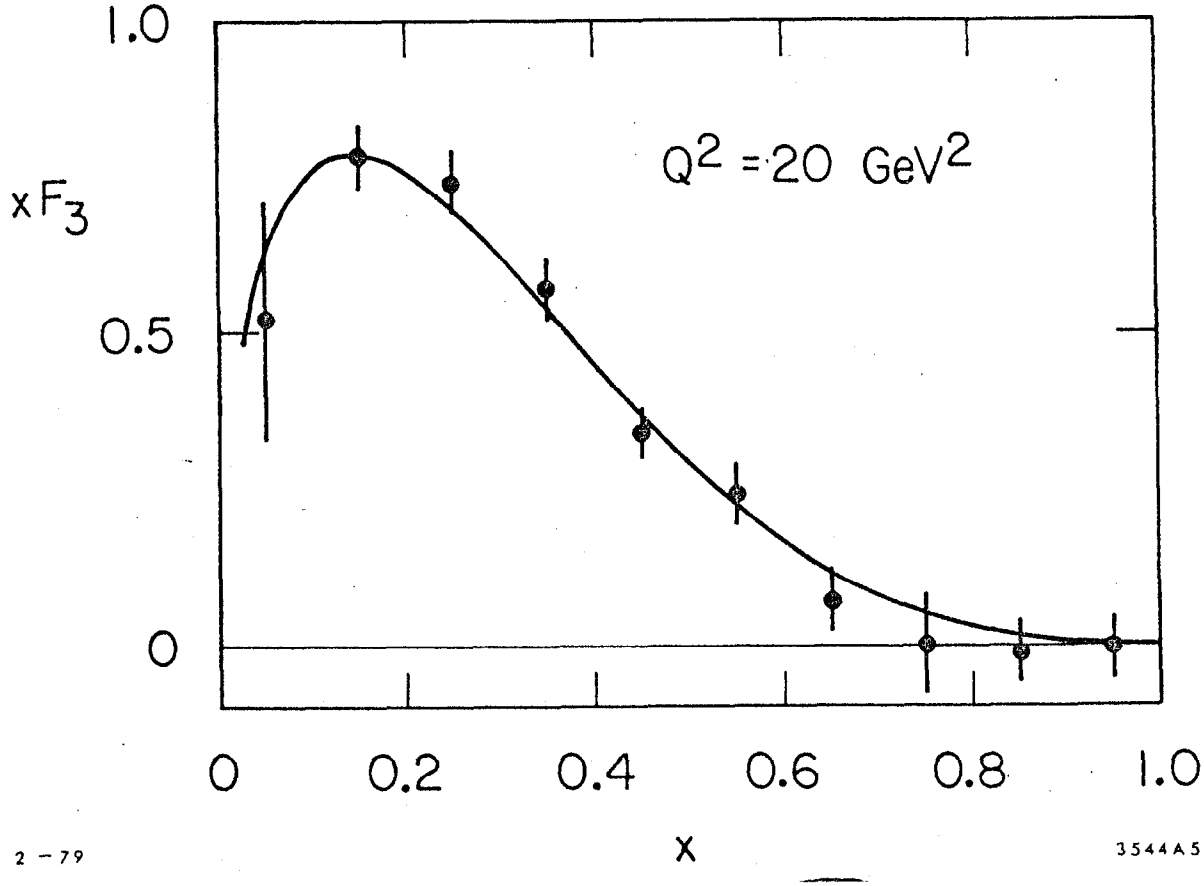

Fig. 1

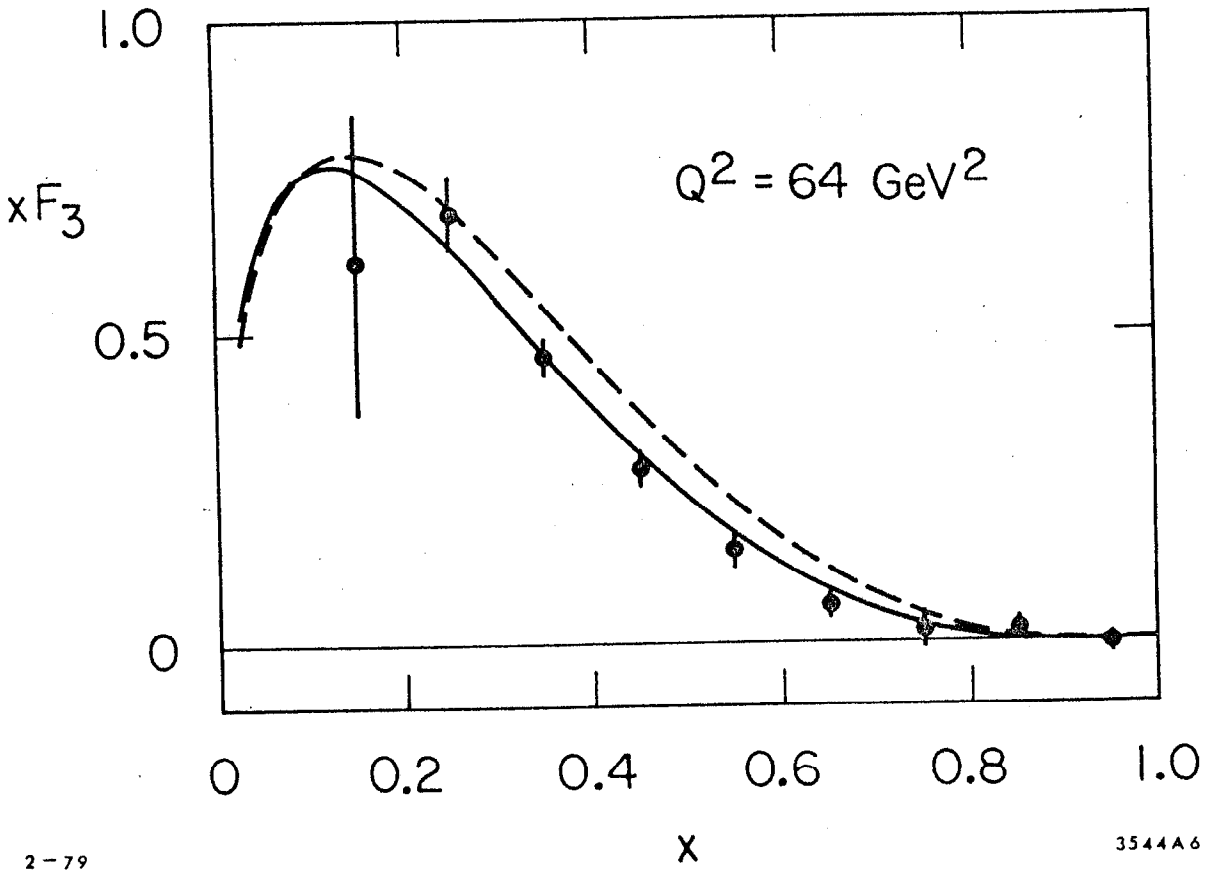

Fig. 2

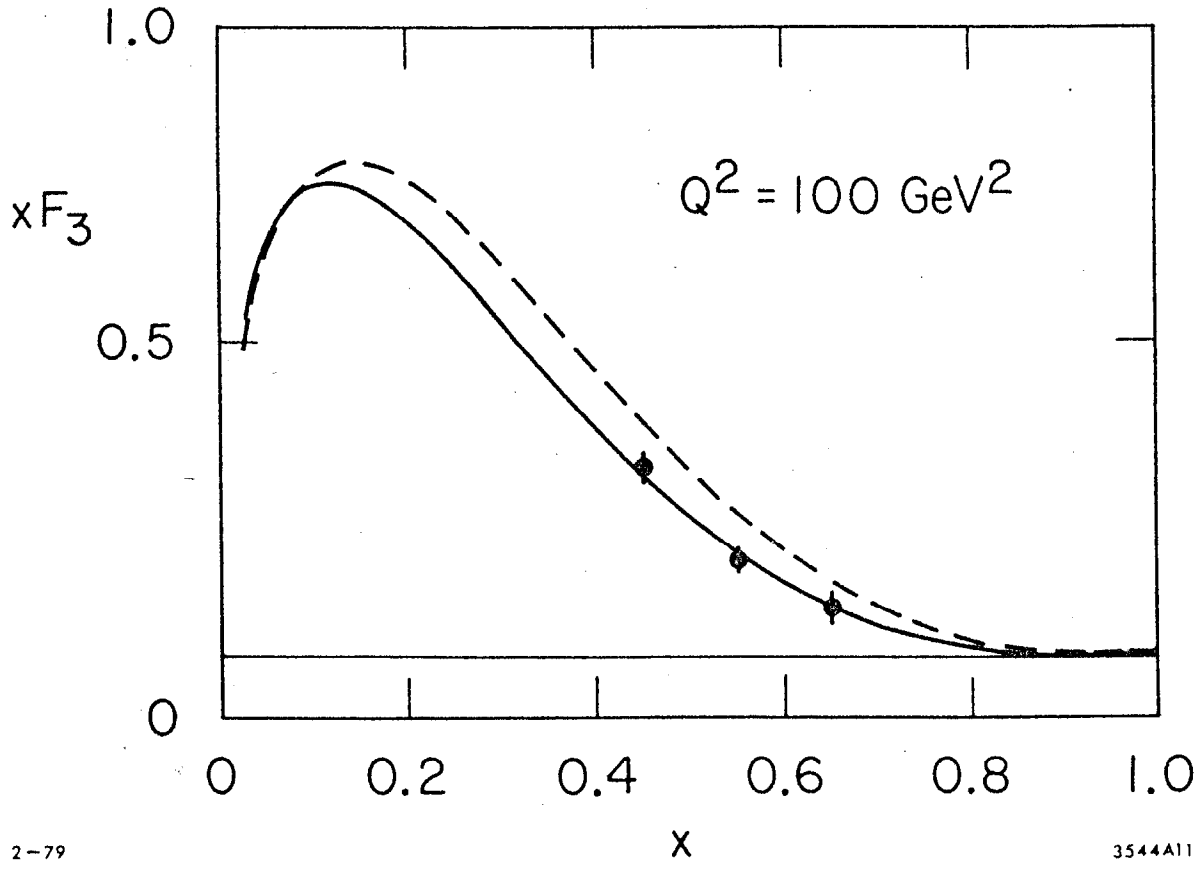

Fig. 3

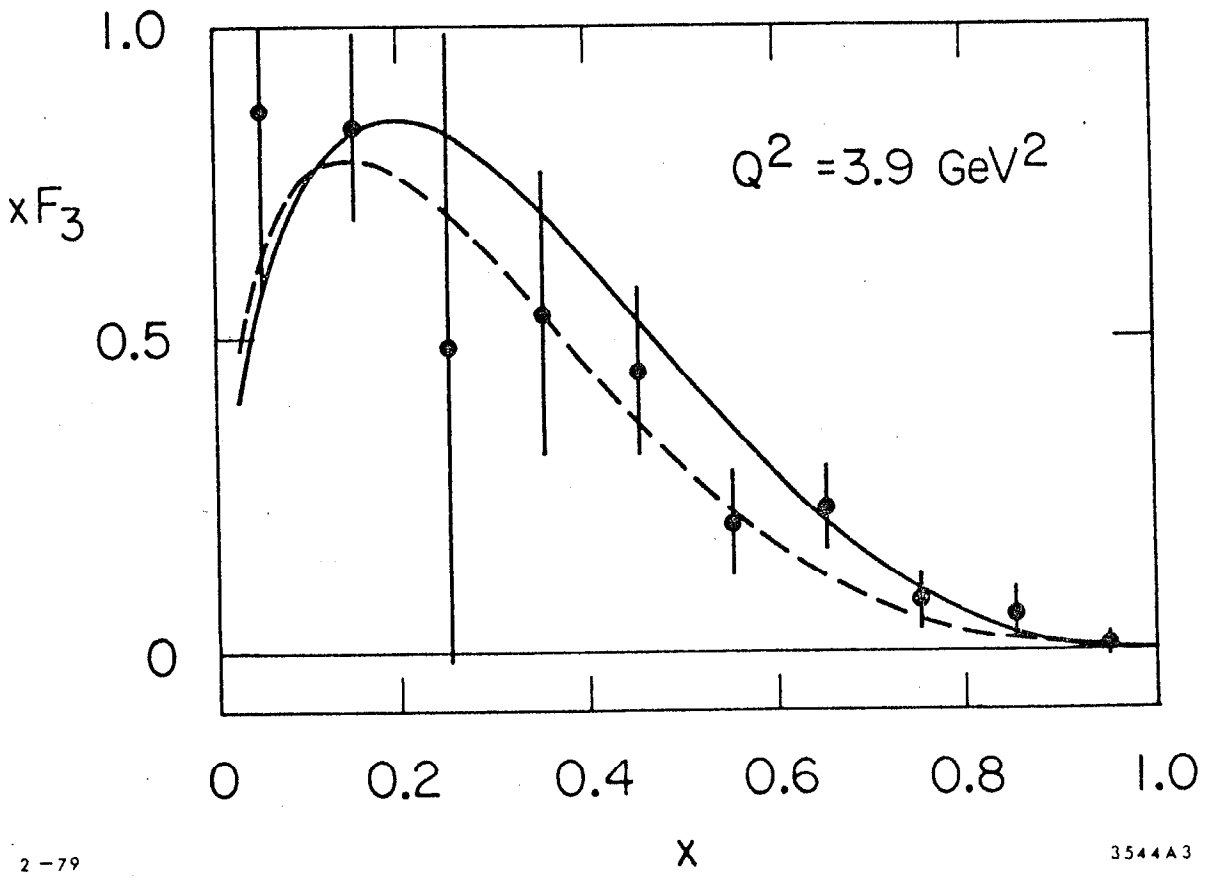

Fig. 4

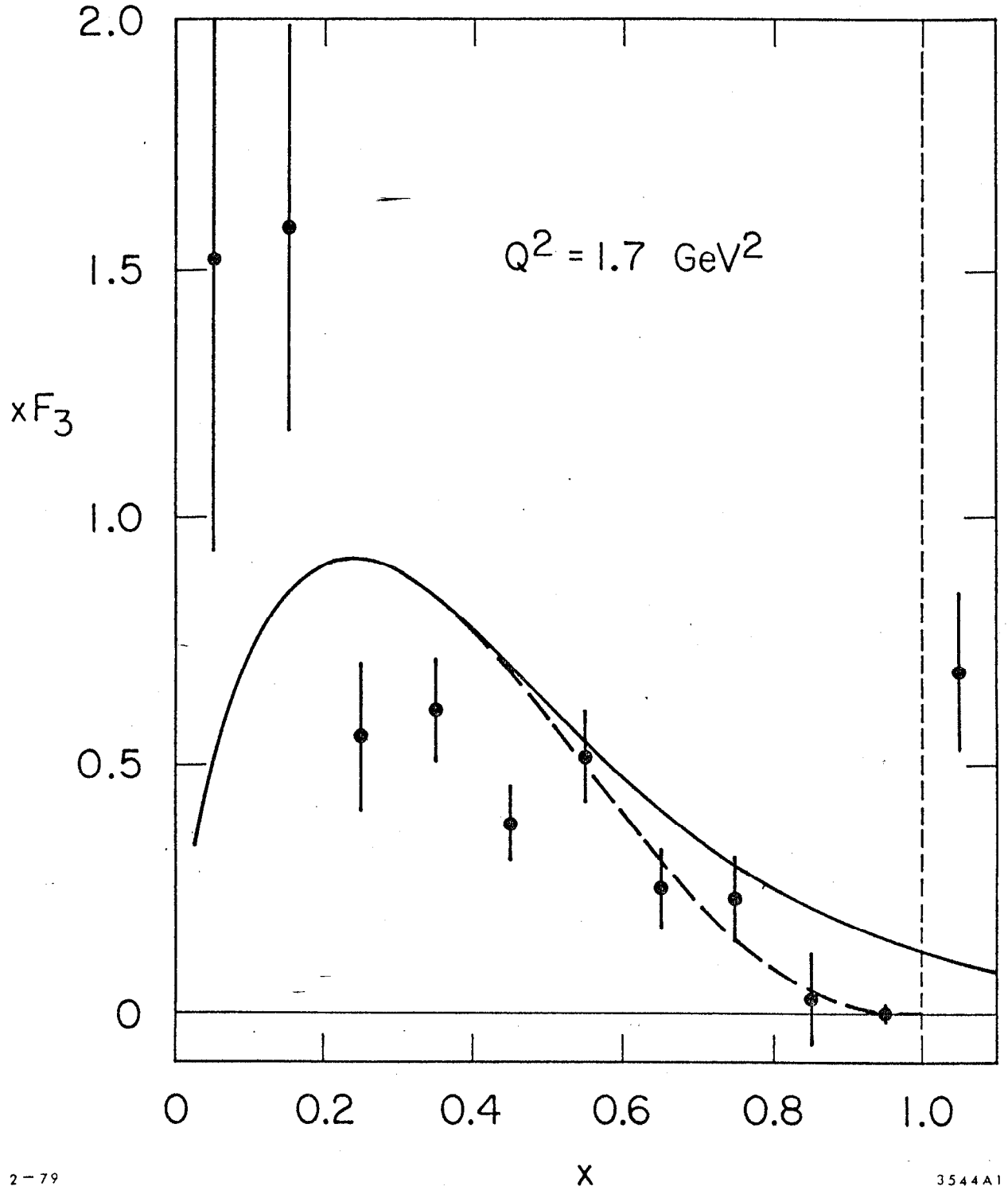

Fig. 5

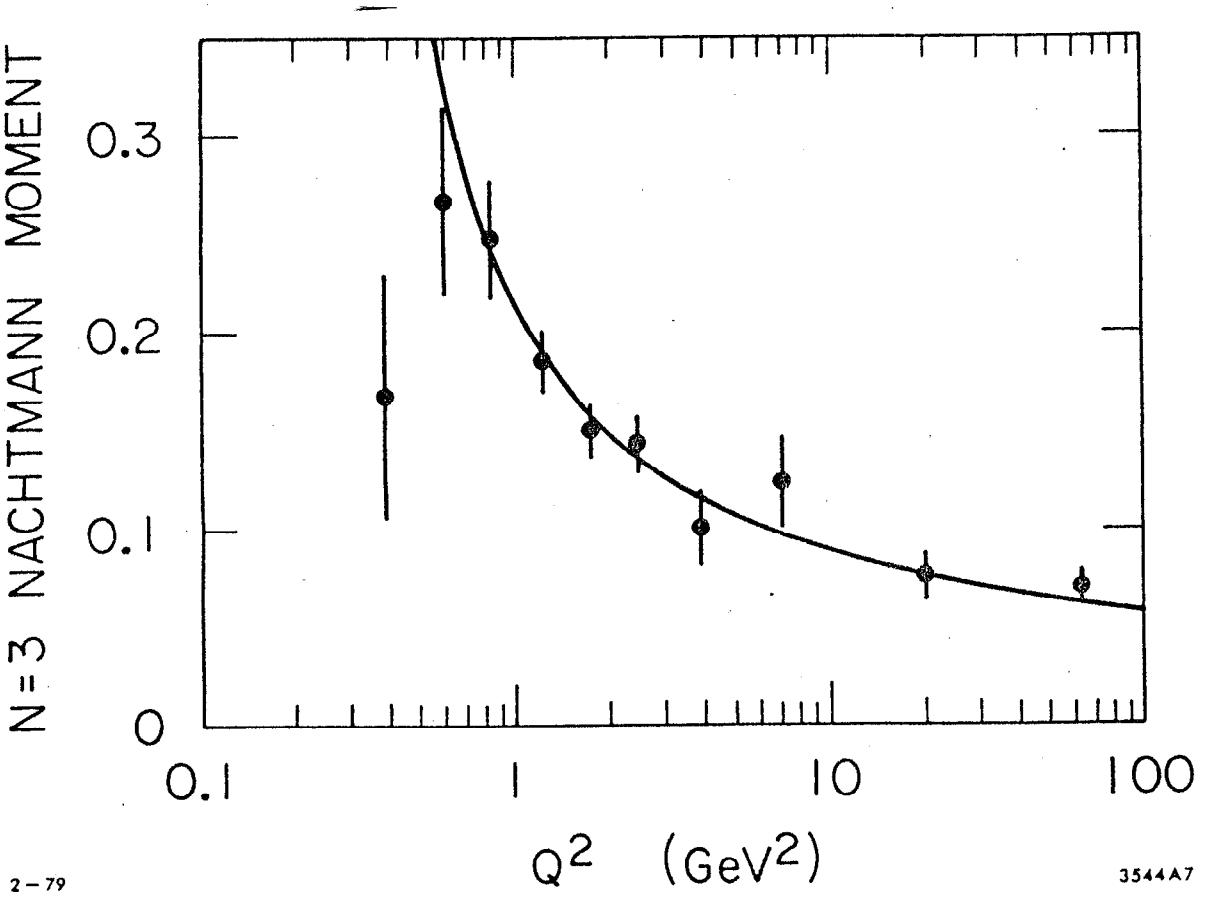

Fig. 6